

Incorporating fire severity for refined data-drive carbon emissions estimates of boreal and temperate forest fires in the Generic Carbon Budget Model (GCBM)

[]¹, ², ³, ¹, ³, and ³

¹
²
³

Correspondence: ()

Abstract. Wildfire is the most impactful natural disturbance to Canada's boreal and temperate forest biomes. Current representations of fire impact on forest carbon stocks is limited to a single parameterization of fire severity (i.e. the fraction of biomass consumed) that assumes only high severity fires, despite a large and increasing evidence base of widespread mixed-severity wildfire. In this submodel of the larger Generic Carbon Budget Model for forest carbon accounting, field measurements of biomass consumption as related to satellite-derived burn severity maps are interpreted from a fire physics and ecology perspective to derive algorithms to describe forest carbon fluxes in the immediate aftermath of fires. Model outputs indicate total carbon emissions range from a 11 t C/ha in Boreal Shield West forests of Saskatchewan following low severity fire to over 70 t C/ha in Taiga Cordillera and Pacific Maritime forests of Yukon under high severity fire. Pacific Maritime forest showed the largest fraction of carbon release in the canopy biomass pools (67%), while Taiga Shield West and Boreal Plains of the Northwest Territories and Manitoba were estimated of having 82% of carbon emissions in the surface and belowground biomass pools of litter, duff, peat, roots, etc.

. His Majesty the King in Right of Canada as represented by the Minister of Natural Resources Canada. This work is distributed under the Creative Commons Attribution 4.0 License.

1 Introduction

Wildfire is on par with insects as the largest stand-replacing disturbance process in Canada's forest, impacting ~1-3 Mha of Canada's 355 Mha forested area in a typical year (Hanes et al., 2019). In Canada's reliable 53-year burned area record, nine years have exceeded 4 Mha of burned area (or approximately 1% of Canada's forest area) (Skakun et al., 2022). The 2023 fire season in Canada burned a remarkable 15 Mha owing to extreme drought, severe fire weather conditions, and a prolonged fire season length (Jain et al., 2024).

20 Of this, managed forest accounts for xxx% of the area burned between 1972 and 2024; publicly-owned managed forest under long-term licence to private timber companies forms 40% of Canada's forest area (Stinson et al., 2019). Privately-owned forest constituting only 6% of the forest area, with the remainder of the forest area being a mix of formally protected areas, remote unmanaged forest, Indigenous reserve lands and other uses without large-scale harvesting. Managed forest areas adjacent to communities have historically shown some local fire suppression effects with a bias towards older forest nearby boreal forest
25 communities in Canada (Parisien et al., 2020), though the effect is limited to a 25 km radius between these widely dispersed communities.

Burned area is dominated by a relatively small number of very large fires, with 3% of fires constituting 97% of the burned area (Stocks et al., 2002). Lightning-caused fires account for approximately half of all ignitions and between xxx and xxxx% of burned area, but no distinction is made between human and lightning ignition for carbon accounting purposes. Annual
30 burned area mapping at 30 metre resolution is conducted using a composite of satellite and aerial mapping; the relatively small number of large fires, and their slow vegetation regeneration (White et al., 2017) allows for reliable mapping using multispectral imagery such as Landsat within one year of the fire (Whitman et al., 2018).

In CBM-CFS, spatially referenced stand lists representing large homogenous stands that fall within spatial units (ecozone-provincial intersections) are randomly (??) drawn (Kurz et al., 2002), even when applying precisely mapped burned areas
35 (Hall et al., 2020). CBM-CFS currently assesses (simulates?, calculates?) fire impacts to carbon pools only as representing high-severity fire, which is the most common of three severity classes of burned forest in Canada (Hall et al., 2008). Biomass consumption estimates are based on the and the assumption of complete crown mortality, with additional biomass consumption following a spatially-referenced aggregated estimate at the ecozone-province of annualized drought conditions.

In Canada's forests, a combination of disturbance history, soils, and less frequently topographic variables determine leading
40 tree species; at local scales (1-100 ha), tree species plays a major role in determining ecosystem susceptibility to fire (Bernier et al., 2016) where older, conifer-dominated forests burn at very high rates relative to adjacent deciduous or mixed stands. Even when deciduous and mixed forests do burn, they do so at consistently lower severity compared to all but the most xeric conifer forests (Whitman et al., 2018). Thus, important biases in fire activity towards older and moderate to poorly-drained forests are not resolved, and only a regionally-averaged fire severity is applied.

45 To support recent advances in operational burn severity mapping for Canada (Whitman et al., 2020) alongside multi-decade reliable burned area records that provide certainty on fire start and end dates (Hall et al., 2020) , the CBM DMs also need to be upgraded.

something about dynamic veg models like landis and how they represent fire disturbance -then how most MRV models and quickly how they do fire disturbance -even a bit on the GFED/GFAS world too

50 that ESSD frames it well, worth reading the intro part in detail) (recent Smyth and Campbell papers too) (other recent Canadian fire-carbon things, Walker - esp is supports consistent patterns in proportional carbon loss)

In this document, we outline the evidence-based fire Disturbance Matrices updated and designed for a spatially-explicit update to the CBM, anchored in a three severity class paradigm. These fire carbon flux models are built from a blend of aggregated field data linked to remotely sensed severity, as well as insights from fire physics and experimental fires. Key

55 knowledge gaps are also highlighted, with interim solutions presented until further quantification can be done in field studies, such as from further wildfire observations, experimental fires, or prescribed fires.

2 Methods

2.1 Biomass pools of the Generic Carbon Budget Model

Short section explaining the pool definitions most relevant to fire.

60 2.2 Axioms of forest carbon budget after fire

To simplify the process of the creation of the DMs as a distillation of the complexities of fire severity and combustion patterns, the following logical axioms are proposed and maintained throughout:

1. Disturbance matrices are to be in terms of mortality, not survival
2. Crown Fraction Burned (CFB) is a mass-based estimate of the portion of foliage consumed in the flaming passage
65 of a fire, and is inclusive of merchantable and submerchantable trees, both broadleaf and needleleaf. Needles that are heat-killed but otherwise not consumed in the fire are not considered part of CFB.
3. The heat-killed but unconsumed fraction of the canopy = (mortality - CFB)
4. In submerchantable trees, mortality = CFB
5. In submerchantable trees, mortality is ≤ 1
- 70 6. In merchantable stands, CFB < mortality
7. Snags are inclusive of both those killed by prior fire as well as those killed by all other causes

Of these, Crown Fraction Burned (CFB) is an important concept used primarily in fire behaviour science but not carbon accounting nor fire ecology. CFB was introduced in the 1992 Fire Behaviour Prediction System documentation (Group, 1992), and provides a simple continuous 0-100 variable for only the consumption of foliage (inclusive of both conifer and broadleaf),
75 as opposed to ordinal and less precise systems like Crown Fire Severity Index that allows the user to specify which pools of canopy biomass are consumed, but not the degree to which a given pool is consumed.

2.3 Ground plot and remotely sensed fire severity data

!!!Ellen to insert methods here - including the figure of where the samples are from etc.

Table 1. Emissions factors in flaming and smouldering phase, expressed as portion of unburned biomass carbon content

Spp	Flaming	Smouldering
CO2	0.868	0.703
CO	0.070	0.161
PM10	0.022	0.048
NMOG	0.016	0.035
PM25	0.019	0.040
CH4	0.005	0.013
BC	0.000	0.000

2.4 Combustion gas emission ratios

80 Certain variables, like the partitioning of CO₂:CH₄:CO gas emissions, are constant throughout ecozones, but vary by flaming vs smouldering combustion modes. They are defined in a global variables table:

85 where CO₂ is responsible for 86.8% of emissions in the flaming phase, but only 70.3% of emissions in the smouldering phase, with a doubling of CO emissions and tripling of CH₄ emissions. With a Global Warming Potential of CO equal to 1.9 and CH₄ of 25, the Global Warming Potential per unit of biomass consumption in the smouldering phase is 1.18 times higher in global warming potential compared to flaming, not including differential aerosol production and injection heights, however. Note that these proposed emissions factors for flaming vs smouldering are aligned with those currently used in Canada's operational wildfire smoke air quality model, FireWork (Chen et al., 2019). With flaming and smouldering each contributing roughly equally to wildfire emissions, these distinct flaming and smouldering emissions rates correspond well with aircraft smoke chemistry observations by (Simpson et al., 2011) and (Hayden et al., 2022) and are themselves very similar to prior 90 emissions factors used in CBM. Note that as current described, the sum of CO₂, CH₄, and CO emissions from wildfires only represent approximately 95% of the fire carbon mass emitted to the atmosphere, with 0.5-2.0% of biomass emitted as particulate matter (e.g. PM2.5, but also PM1 and PM10 classes of particulates at 1 and 10 um diameters, respectively), and an additional 3% (Hayden et al., 2022) to as little as 1% (Simon et al., 2010) composed of non-methane organic gases that have a large range in global warming potentials as compared to CH₄.

95 2.5 Litter layer area-wise consumption by severity class

The litter layer forms the first biomass pool in which a spreading fire consumes fuel. In low-severity fires, the litter layer may be consumed little to no underlying duff material consumed, nor any tree mortality (Hessburg et al., 2019). Logically, since litter consumption is required for the ignition of the underlying duff layer, this litter area-wise fractional consumption also informs and constrains duff consumption.

Table 2. Unburned litter area by ecozone and severity class. The majority of the data comes from studies in the Boreal Plains and Boreal Shield West, and so values are extrapolated from those two well-observed ecozones to all others.

Ecozone	Low	Mod	High
BSW	0.20	0.08	0.05
TP	0.14	0.16	0.03
TSW	0.20	0.08	0.05
BP	0.14	0.06	0.02
BC	0.14	0.06	0.02
BSE	0.20	0.08	0.05
TSE	0.20	0.08	0.05
MC	0.14	0.06	0.02
HP	0.20	0.08	0.05
TC	0.14	0.06	0.02
PM	0.14	0.06	0.02
AM	0.14	0.06	0.02
MP	0.14	0.06	0.02
P	0.14	0.06	0.02

100 2.6 Duff Consumption

While consumption of fine fuels in the litter layer of the forest floor is nearly complete for any given fire intensity, consumption of deeper organic soil horizons (F+H layers in upland forests and upper peat layers in wetlands) is more drought dependent. In the fire literature in Canada, the soil organic layer is termed Forest Floor Fuel Load (FFFL) and is dominated by the equivalent Belowground Slow pool (BGSslow) in CBM. Typically attention has been paid to the absolute value of Forest Floor Fuel 105 Consumption (FFFC); however in the case of carbon modelling, it is the relative fraction of consumption (FFFC/FFFL) that is of interest. In this scheme, we utilize a composite of wildfire data from (de Groot et al., 2009) alongside the ABoVE duff consumption data , with an alternative modelling approach to compute the relative amount of depth of consumption (scalar from 0 to 1) rather than an absolute value in kg m^{-2} or cm as otherwise done in the literature. A logit transform is used on the scalar data to make it suitable for the fitted non-linear least-squares modelling:

$$110 \quad \text{logit} \left(\frac{\text{depthofburn}}{\text{prefiredepth}} \right) = [3.83(1 - e^{(-0.005DC)})] + (-0.718\log_e(\text{BGSslow})) \quad (1)$$

where DC is the Fire Weather Index Drought Code, and BGSslow in the CBM (given in Mg C/ha in this equation), and also synonymous with the the Forest Floor Fuel Load (with ecozone averages given in (Letang and de Groot, 2012) or site-level data

where observed). The modelling of relative depth of burn had a higher skill than modelling of the relative mass of consumption, given natural variability in soil density with depth.

115 A conversion factor is then applied to the relative depth of burn data to convert it to a relative mass consumption value. Since organic soil density always increases with depth, this conversion factor from depth to mass is less than one:

$$\left(\frac{\text{massconsumed}}{\text{prefiremass}} \right) = \left(\frac{\text{depthofburn}}{\text{prefireddepth}} \right) * CF \quad (2)$$

where the Correction Factor is defined for boreal spruce fuel types as:

$$CF_{spruce} = 1.018(RelativeDepth)^{0.250} \quad (3)$$

120 and for all other fuels as

$$CF_{nonspruce} = 0.13(RelativeDepth) + 0.87 \quad (4)$$

with RelativeDepth as a value from 0-1.

While ultimately this scheme can be used on individual fires with estimated or measured fuel loading and specific Drought Code values, for the purposes of this first assessment, an ecozone-averaged fuel load and decadal composites of Drought Code 125 can also be used to provide representative values. Specifically, a median Drought Code of detected fire hotspots in Canada from 2003-2021 (Barber et al.) using the same data as the Canadian CFEEPS-FireWork wildfire air quality model of (Chen et al., 2019) is presented below, along with proportional consumption values of the forest floor by ecozone:

Note that the maximum upland Forest Floor Fuel Load is approximately 30 kg m⁻² (Letang and de Groot, 2012); higher values are typically seen only in peat ecosystems, where the above Forest Floor Fuel Consumption scheme does not apply. For 130 Canadian peatlands, the CaMP model (Bona et al., 2020) is instead used in CBM. Within CaMP, a separate peatland water model driven by Drought Code determines the thickness of the unsaturated peat layer, and an amount approximating 12% of the thickness of the unsaturated peat is consumed as smouldering consumption. The peat-specific carbon pools and fire Disturbance Matrices are fully described in (Bona et al., 2020); large peatland trees will still utilize the DM scheme described below.

135 Little data is available on the fraction of woody debris consumption alongside fire severity measurements. Coarse woody debris of overstory stems that makes up 60-80% of woody debris biomass in Canada's boreal and temperate forests (Hanes et al., 2021), with its moisture and consumption patterns largely follows the moisture regime of the Drought Code (McAlpine, 1995). In this modelling framework, the proportion of coarse (>7.5 cm diameter) and medium (>0.5 cm and <7.5 cm) woody debris consumption is estimated based on detailed measurements of consumption from experimental fires. Coarse Woody 140 Debris is responsible for approximately 50-75% of the total woody debris load in most ecozones, and approximately 60% of the total woody debris consumption. Ecozone-level CWD consumption rates are summarized as:

Table 3. Fire Weather, fuel loading, and duff consumption values per ecozone

Ecozone	Median Drought Code of Burning	Median FFFL kg m-2	FFFC kg m-2	% consumption
BSW	239	8.8	3.7	0.42
TP	369	15	7.01	0.47
TSW	297	1.7	1.33	0.78
BP	242	9.8	3.96	0.4
BC	250	8.31	3.72	0.45
BSE	123	10.9	1.95	0.18
TSE	98	1.7	0.71	0.42
MC	452	6	4.15	0.69
HP	204	7.9	3.02	0.38
TC	254	8.31	3.77	0.45
PM	268	15.2	5.45	0.36
AM	270	10.9	4.62	0.42
P	242	9.8	3.96	0.4

Table 4. Coarse Woody debris consumption rates from pre/post measurements in experimental fires

Ecozone	Low	Mod	High
BSW	0.024	0.163	0.140
TP	0.000	0.218	0.238
TSW	0.000	0.218	0.238
BP	0.359	0.509	0.412
BC	0.024	0.163	0.140
BSE	0.080	0.131	0.182
TSE	0.080	0.131	0.182
MC	0.024	0.163	0.140
HP	0.080	0.131	0.182
TC	0.024	0.163	0.140
PM	0.024	0.163	0.140
AM	0.080	0.131	0.182
MP	0.080	0.131	0.182
P	0.359	0.509	0.412

Table 5. Softwood fractional mortality by ecozone, as derived from median values from field studies

Ecozone	Low	Mod	High
BSW	0.45	0.81	1.00
TP	0.45	0.81	1.00
TSW	0.10	0.81	1.00
BP	0.45	0.81	1.00
BC	0.24	0.65	0.98
BSE	0.45	0.81	1.00
TSE	0.10	0.81	1.00
MC	0.28	0.74	0.98
HP	0.45	0.81	1.00
TC	0.24	0.65	0.98
PM	0.13	0.38	0.97
AM	0.28	0.34	0.95
MP	0.28	0.34	0.95
P	0.45	0.81	1.00

Note that where historical burn severity data is not available, and instead the fire classification type of surface, intermittent crowning, and active crown fire are used as proxies for low, moderate, and high severity fire, respectively. Fine woody debris <0.5 cm in diameter is consumed at the exact same rate as the litter pool (see section above).

145 2.7 Drivers of C losses in the tree canopy

2.7.1 Overstory tree mortality and consumption

Numerous process-driven (Michaletz and Johnson, 2006) or empirical (Hood and Lutes, 2017) tree mortality models are present and show significant skill in predicting tree mortality based on fire behaviour (i.e. flame length, rate of spread). Since the driving data in this model is satellite-derived fire severity over the landscape scale, fire behaviour metrics such as flame length 150 or scorching height of bark are not available as a continuous mapped product. Instead, softwood and hardwood overstory mortality is calculated per ecozone as a function of satellite-observed fire severity using aggregated ground plot data:

And since large-diameter, live trees killed by fire do not experience significant live stemwood consumption, the entirety of the live stemwood biomass pool that is killed is transferred to the snag pool. Note that the field data and disturbance modelling undertaken here only accounts for tree mortality within the calendar year of the fire, and delayed mortality of over one year has 155 been documented in boreal low and moderate severity fires (Angers et al., 2011) where less than half of total mortality occurs after the year of the fire. Thus, the modelling here does not account for delayed mortality that may extend upwards of 5 years after fire.

Table 6. Softwood crown fraction burned by ecozone, as derived from median values from field studies

Ecozone	Low	Mod	High
BSW	0.0	0.81	1.00
TP	0.0	0.81	1.00
TSW	0.1	0.81	1.00
BP	0.0	0.81	1.00
BC	0.0	0.65	0.98
BSE	0.0	0.81	1.00
TSE	0.1	0.81	1.00
MC	0.0	0.74	1.00
HP	0.0	0.81	1.00
TC	0.0	0.65	1.00
PM	0.0	0.38	0.97
AM	0.0	0.34	0.95
MP	0.0	0.34	0.95
P	0.0	0.81	1.00

Crown Fraction Burned (CFB) speaks to the fraction of the live canopy that is itself consumed in the flaming front. The alternate outcomes being survival of the foliage, or the mortality of the tree without canopy consumption, resulting in the dropping of foliage onto the forest floor. From the axioms stated earlier, the CFB must be lower than or equal to the mortality rate, using field studies that show any partial crown consumption is likely sufficient to result in high rates if not complete mortality (Hood and Lutes, 2017), which is the case in Canada's trees with primarily thin bark. Due to the structure of the CBM, all High Severity fires have their mortality in the merchantable and smaller trees set to exactly 1.0, which is no more than a 5% variance from observed values. From field studies, the following ecozone-specific CFB values are found:

The consumption of live bark biomass is a pool in the model, and consumption rates can be defined by severity class. At the moment, lacking robust field data on bark biomass consumption rates across ecozones and severity classes (which are a small portion of the overall biomass), the bark proportional consumption rate is set to 34% of the overstory mortality rate, based only on a single set well-observed high severity fires in the Taiga Plains by [santín2015].

A major distinction is made between softwood and hardwood trees, where in Canada's boreal forests, a large fraction of hardwood trees (see Appendix E) are able to resprout even when the main stem has been killed by an intense forest fire (Brown and DeByle, 1987). Accordingly, the root mortality rates differ greatly between softwoods and hardwoods, with softwood root mortality equal precisely to stem mortality, while in resprouting hardwoods, little root mortality is observed even after intense fire (Pérez-Izquierdo et al., 2019). Though GCBM can resolve a species list down to the pixel level, currently an ecozone-level regional average composition of hardwood species with resprouting traits is used and is shown below:

Table 7. Ecozone-level average fraction of hardwood overstory species that do not suffer extensive belowgroud biomass mortality after fire

Ecozone	Resprout Fraction
BSW	0.75
TP	0.75
TSW	0.94
BP	0.99
BC	0.76
BSE	0.67
TSE	0.78
MC	0.97
HP	0.80
TC	0.27
PM	0.39
AM	0.76
MP	0.32
P	0.99

175 Concurrently, the fraction of fine roots contained within the combustible forest floor layers can be a close to or exceeding 50% of the fine root biomass (Strong and La Roi, 1985), and burns alongside the organic soils (Benscoter et al., 2011). As a result, the calulation for softwood fine root consumption and mortality are as follows, using Softwood as an example:

$$SWFineRootConsump = SW.Mort \times SW.Prop.Fine.Root.duff \times Duff.Consump.Fract \quad (5)$$

$$SWFineRootMort.AG = SW.Mort \times SW.Prop.Fine.Root.duff \times (1 - Duff.Consump.Fract) \times (1 - ReSproutFactor) SWFineRootConsump \quad (6)$$

180 In contrast, the larger diameter of the coarse root biomass pool prevents its consumption during any smouldering of the duff layer, and the mortality rate of coarse roots is simply proportional to that of the stemwood overall.

2.7.2 Understory tree mortality and consumption

Understory (or small diameter overstory) tree mortality is defined seperately in the model, but given the lack of data on diameter classes in the severity data, robust field data on differing mortality rates of smaller diameter trees is not available, and so the 185 understory tree mortality rate is set equal to the overstory rate as defined in the table above. Note that trees with a top height less than 1.4 m are not considered in this pool, and instead are lumped into the “other” pool.

2.7.3 Snag and stump consumption

Compared to live stemwood of the same diameter, the low moisture content of standing dead stemwood (snags) allows for much greater consumption during the passage of an intense flaming front. The snag branch pool experiences almost complete
190 combustion, while the largest biomass pool of the main standing dead stemwood

2.8 Construction fire disturbance matrices

Give total number of global parameters, and parameters per ecozone, and then total parameters, and what % of total parameters we have so far filled with data

2.9 Calculation of Annual Direct C Emissions from Fire

195 To compute an estimate of the total direct C emissions from forest fires in Canada in 2023, the classified burn severity product from the National Burned Area Composite annual production was utilized (see Hall et al 2020 for an algorithm description). In NBAC, an internal tracking value “NFIREID” is utilized, which is the final satellite-derived burned area polygon (allowing for multi-part polygons) is split across any RU unit boundaries (if any). Since carbon pool sizes vary across RU boundaries, this allows for a single NFIREID to be present across multiple RUs.

200 A total of 2199 fires as small as 0.09 ha (one 30x30 landsat pixel) were mapped by NBAC for burn severity for a total of 14.60 Mha, but only fires over 100 ha were utilized as a lower limit of where meaningful per-fire estimates of the fraction of low, moderate, and high severity burned area was available. Including only fires 100 ha and larger reduced the total number of fires to 966 but the total area remained largely the same at 14.58 Mha. A total of 189,704 ha of post-fire salvage logging was also mapped in 2023 and is assigned to the moderate severity class after consultation with provincial land managers. The direct
205 C emissions from fire shown here are not altered by the act of post-fire salvage logging. Additionally, the NBAC mapping process accounts for unburned islands (and areas with a mapped fire severity no different than unburned) which count towards the total fire area but do not have a disturbance matrix and direct C estimate applied.

A unique DM was then calculated for each fire using the median area-weighted Drought Code per fire. All thermal detection hotspots from VIIRS that intersect a fire were extracted from the historical hotspot archive that supports the Canadian smoke
210 emissions model CFFEPPS-FireWork (Chen et al., 2019). The median DC value across all intersecting hotspots was used to derive a single DM per fire, no matter the duration of burning (could show first and last hotspot as a figure?).

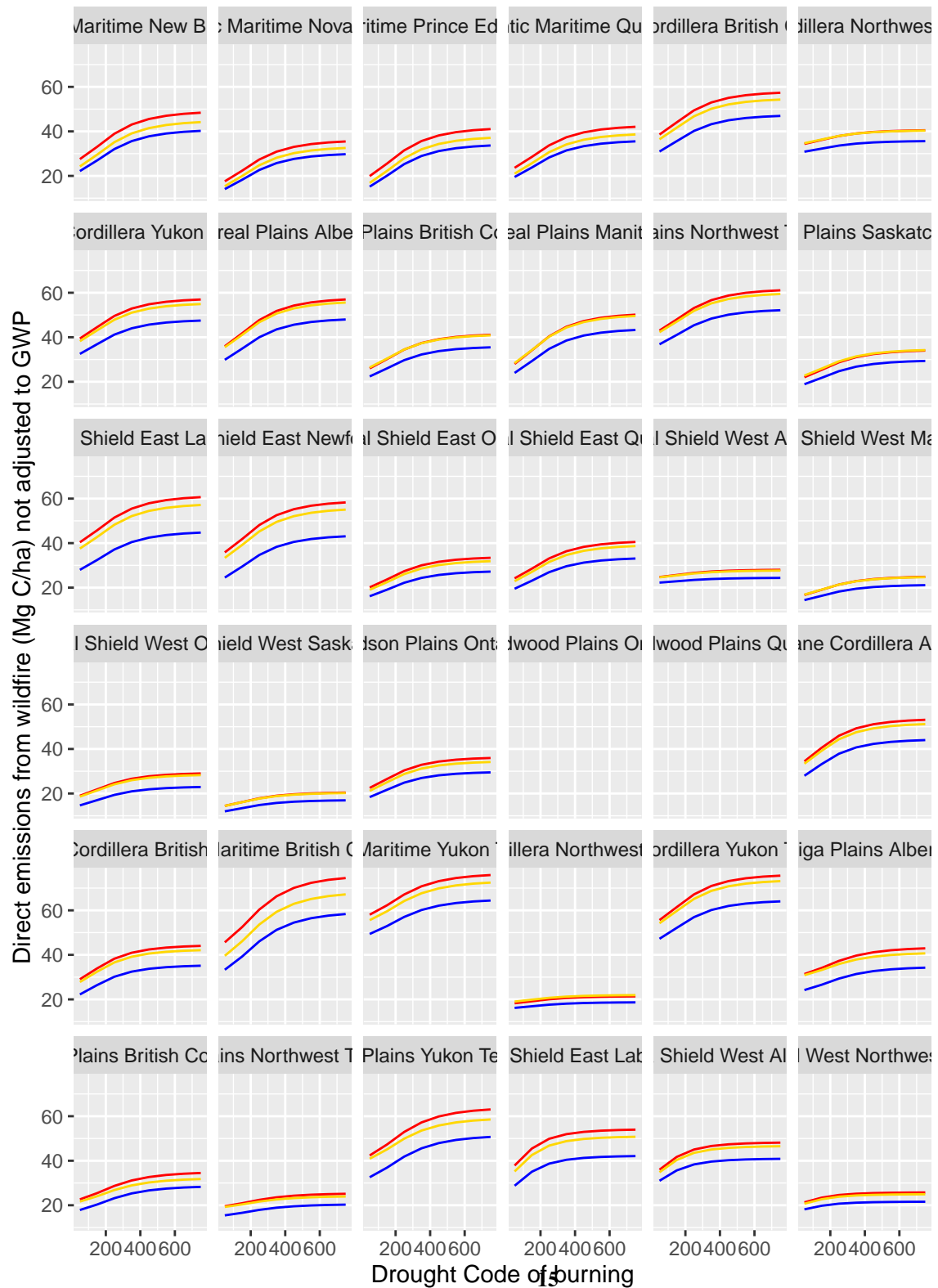
To compute total direct fire emissions per fire, a single estimate of the carbon pool size based on the Reconciliation Unit of the centroid of the NFIREID polygon was applied. Since polygons are split across RU boundaries, the spatial weighting of the pool size per fire is performed automatically. While spatially explicit biomass maps are available for some aboveground
215 components (SCANFI) and some belowground components (Hanes), the majority of the required pool sizes in CBM for the computation of the fire DMs are available only at the spatially referenced RU scale.

3 Results

Table 8. High severity Disturbance Matrix in BP

	Softwood Merchantable	Softwood Stem Snag	Medium DOM	Softwood Foliage	Aboveground Very Fast DOM	CO2	CH4	CO	PM25
Softwood Merchantable	0	1							
Softwood Stem Snag		0	0.90000			0.0868000	0.0005000	0.0070000	0.0019000
Medium DOM			0.57624			0.2979033	0.0055089	0.0682254	0.0169504
Softwood Foliage				0	0.00	0.8680000	0.0050000	0.0700000	0.0190000
Aboveground Very Fast DOM					0.02	0.8506400	0.0049000	0.0686000	0.0186200
CO2									
CH4									
CO									
PM25									

3.1 Direct fire carbon emissions as a function of fire severity and drought



Direct emissions by severity class: red = high, yellow = moderate, blue = low severity

Table 9. Comparison of the Modified Combustion Efficiency (MCE) of airborne gas measurements of Canadian wildfires against modelled MCE

Study	Date	Subset	Ecozone	Drought Code	Obs MCE	Modelled MCE
Hornbrook et al 2011	2008-07-01	Afternoon (0.2Low 0.4Mod 0.4High)	Boreal Shield West	250	0.92	0.908
Hornbrook et al 2011	2008-07-01	Late Evening (100% low severity)	Boreal Shield West	250	0.82	0.903
Hornbrook et al 2011	2008-07-04	After rain smouldering only low severity	Boreal Shield West	275	0.83	0.903

220 3.2 Comparison against observed fire gas emissions

3.2.1 Forest fire observations of CO and CO₂ emissions ratios

-discussion: MCE modelled here fits well against obs MCE during peak burn periods, but does not represent smouldering-only periods such as night-time and after small rain events

3.2.2 2023 Canadian wildfire season total emissions

225 – paragraph on extended impacts like delayed stem mortality, rapid snag fall, and changes (or not) in duff decomposition rates. Not (as of yet) covered in this 1-timestep pulse disturbance described here.

-future work on biomass maps in GCBM will improve this emissions estimates only marginally, since during large fire years with drought such as 2023 there is little fuel selection bias in burned area. # Conclusions

The conclusion goes here.

230 4 Appendix A: list of fluxes and corresponding fire-related plain-language summary.

5 Appendix B: non-linear least squares modelling of soil organic layer consumption

For national annual estimates of forest organic soil layer consumption during wildfire, implementations that only utilize Canadian experimental fire data from the Fire Behaviour Prediction System will be limited to a maximum consumption value of 5 kg/m² of total surface fuel (woody debris, litter, and duff) of 5 kg/m², or 25 Mg C/ha, given the observation dataset and 235 fitted model parameters. For the common C-2 Boreal Spruce fuel type for instance, Surface Fuel Consumption (kg m²) is modelled as:

$$SFC = 5.0 \left(1 - e^{-0.0115 BUI}\right)^{1.0} \quad (7)$$

This model form has the distinct advantage of SFC being 0.0 at a BUI of zero. The model parameters vary by fuel type (i.e. deciduous broadleaf fuels are limited to 1.5 kg/m² of maximum SFC) but are fixed within a fuel type.

240 More recent observations and modelling from de Groot et al. (2009) extended the FBP data with an additional 128 observations
 from 7 additional wildfires, and the ABoVE project compiled over 1000 field observations of depth of burn and C stocks before
 and after wildfire in Canada and Alaska, over 600 of which are in North American Level II ecoregions also occurring in Canada
 (fix Walker 2020 ORNL DAAC ref in bibtex here). de Groot et al. (2009) provides a concise and informative improvement on
 the FBP fuel consumption equations, where both a Fire Weather Index System component (in this case, Drought Code) is used
 245 similarly to Buildup Index in the FBP, but importantly, the site-level organic soil layer fuel load is also accounted for, which
 allows for the greater absolute combustion in deeper organic soils that is moderated by the natural logarithm transformation:

$$\log_e(FFFC) = -4.252 + 0.710\log_e(DC) + 0.671\log_e(FFFL) \quad (8)$$

where FFFC is Forest Floor Fuel Consumption (SFC minus surface woody debris) in kg m² and FFFL is Forest Floor Fuel Load in kg/m². This model fits well within the dataset and extends the observed maximum FFFC to nearly 10 kg/m². The
 250 ABoVE synthesis of FFFL and FFFC (Walker et al 2020 ORNL) expands upon a slightly smaller dataset used in a modelling
 summary also by Walker et al (2020 NCC), where structural equation modelling was used to explore drivers of FFFC but no
 concise and readily reproducible modelling is produced. The results of the SEM from Walker et al (2020 NCC) emphasized a
 greater role of FFFL over DC, though coarse reanalysis that lacked local fire agency weather stations was used. An analysis
 255 of just 2014 fires in the Northwest Territories by (walker2018) showed that while the mean depth of burn across all black
 spruce stands was 6-10 cm, the driest (xeric) black spruce stands with the smallest FFFL showed upwards of 75% soil organic
 consumption, while deeper organic soils in subhygric black spruce stands showed less than 25% consumption.

To provide the largest possible dataset for FFFC and FFFL, the ABoVE synthesis was combined with wildfire data from
 de Groot et al 2009 not otherwise found in the ABoVE synthesis. The ABoVE synthesis sites in the Alaska Boreal Interior
 ecoregion, which have equivalent Canadian ecozone were excluded, but Alaska Boreal Cordillera sites near the Yukon border
 260 were utilized. Experimental fire data from the FBP data was not used, as deeper combustion measurements resulting from
 hours and days of smouldering combustion captured in wildfire data are not available in experimental fires where extensive
 smouldering is not measured due to suppression. In order to best represent on-the-ground Fire Weather Index values, the
 Drought Code and other FWI values from Walker et al 2020 reanalysis were substituted with interpolated weather station
 265 (both Environment and Climate Change Canada as well fire agency stations). This data also has the benefit of being properly
 overwintered for Drought Code (Hanes DC overwinter) and capturing small rain events not captured in reanalysis that meaningfully
 impact the Duff Moisture Code in particular.

For the purposes of improving national estimates of the fractional soil organic layer loss during wildfire, this framework
 emphasizes the proportional C stock loss (as with all CBM disturbance matrices) rather than the absolute value of combustion.
 In contrast to the modelling of absolute combustion value, any analysis of proportions is best conducted as logit- transformed
 270 data, where the logit transformation is:

$$\text{logit}(p) = \log \frac{p}{1-p} \quad (9)$$

which effectively transforms a data of proportions of [0,1] to a Gaussian distribution with a range of approximately -5 to +5 (in this dataset), and a mode approximately at zero. Within the logit-transformed data, exploratory analysis of ecozones as a factor alongside other non-linear splines of FWI values and FFFL was conducted:

```

275  ##
  ## Family: gaussian
  ## Link function: identity
  ##
  ## Formula:
280  ## prop_sol_combusted_logit ~ s(drought_code, k = 4, bs = "tp") +
  ##     ecozone + s(BGSlow.Mg.C.ha, k = 4, bs = "tp")
  ##
  ## Parametric coefficients:
  ##             Estimate Std. Error t value Pr(>|t|)
285  ## (Intercept) 0.11939   0.09318   1.281  0.2005
  ## ecozoneBP   -0.29433   0.15506  -1.898  0.0581 .
  ## ecozoneBSW  -0.19928   0.15988  -1.246  0.2131
  ## ecozoneTP   -0.23049   0.11476  -2.008  0.0450 *
  ## ecozoneTSW  -0.29887   0.12157  -2.458  0.0142 *
290  ## ---
  ## Signif. codes:  0 '***' 0.001 '**' 0.01 '*' 0.05 '.' 0.1 ' ' 1
  ##
  ## Approximate significance of smooth terms:
  ##             edf Ref.df      F p-value
295  ## s(drought_code) 1.352  1.618  2.862  0.0631 .
  ## s(BGSlow.Mg.C.ha) 2.950  2.998 232.720 <2e-16 ***
  ## ---
  ## Signif. codes:  0 '***' 0.001 '**' 0.01 '*' 0.05 '.' 0.1 ' ' 1
  ##
300  ## R-sq. (adj) = 0.628 Deviance explained = 63.3%
  ## -REML = 869.04 Scale est. = 0.81207 n = 651

```

(could also show boxplots?) which shows that the Boreal Cordillera ecozone has a meaningfully higher proportional soil organic layer consumption rate compared to BP, BSW, TP, and TSW, all of which are not significantly different in consumption rates once DC and FFFC (shown as BGSlow.Mg.C.ha) are accounted for. Boreal Cordillera data were set aside for a distinct model.

Similar to de Groot et al. (2009), Drought Code was a better predictor of consumption rates than Buildup Index as used in the FBP. In the logit transformed space, saturation-type non-linear curve using the relevant FWI component was fitted in a non-linear least squares model, but an additive term of the natural-logarithm transformed FFFC (given as BGSlow pool in Mg C/ha) was used as well. In the end, a superior model was found using the proportional depth of burn, rather than the proportional loss of the mass of the soil organic layer. The non-linear least squares model fit was conducted using the Levenberg-Marquardt nonlinear least-squares algorithm found in MINPACK (Elzhov et al 2023) R package, which supported bounded parameter constraints.

In the abstract, the model follows the form:

$$\text{logit} \left(\frac{\text{depthofburn}}{\text{pre - fireorganicdepth}} \right) = [c(1 - e^{(aDC)})] + (b \log_e(\text{BGSlow})) \quad (10)$$

with fitted parameters as:

$$\text{logit} \left(\frac{\text{depthofburn}}{\text{pre - fireorganicdepth}} \right) = [3.83(1 - e^{(-0.005DC)})] + (-0.718 \log_e(\text{BGSlow})) \quad (11)$$

Note the “b” coefficient on the parameter associated with the FFFL (BGSlow) of -0.718, which results in larger organic layer fuel loads leading to smaller proportional consumption values, which follows the patterns shown by Walker 2018 for NWT fires of 2014.

The a parameter term that forms the exponent of e alongside Drought Code is related to the DC value at which half of the maximum possible asymptotic consumption value is observed (for a given FFFL value). The NLS fitting was given a minimum value of -0.06 such that half of the asymptotic maximum consumption rate was modelled as occurring at or around a DC value of 300. The other parameters were fit to the best possible value with no constraint.

Importantly, since fire behaviour, emissions modelling, and carbon accounting all operate with the calculation of mass loss and depth of burn, a correction factor was applied that corrects for the trends in bulk density with depth for C-2 fuels as given by de Groot et al. (2009), so that a model of proportional depth of burn is then converted into a proportional mass loss term:

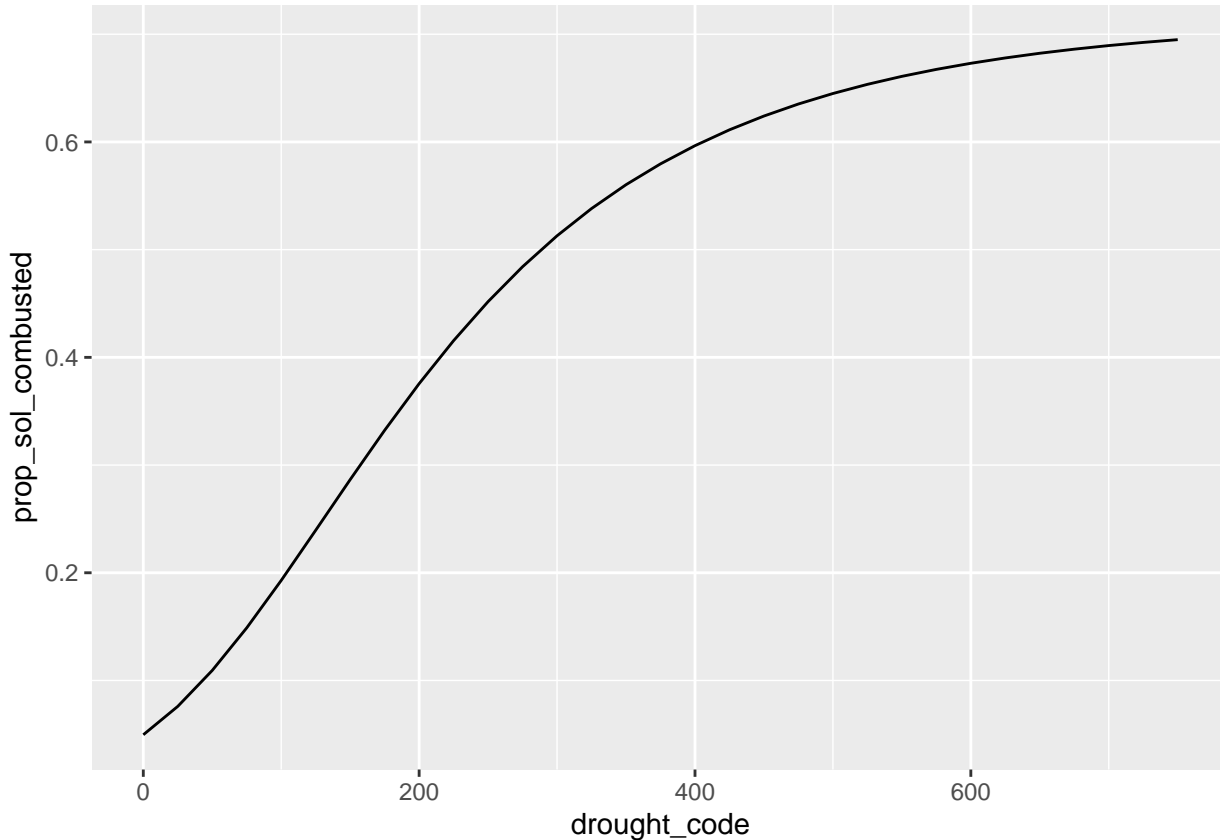
$$\left(\frac{\text{FFFC}}{\text{FFFL}} \right) = 1.017 \left(\frac{\text{depthofburn}}{\text{pre - fireorganicdepth}} \right)^{0.250} \quad (12)$$

which for example means that the median proportional depth of burn in the AboVE/de Groot training data of 0.40 corresponds to 0.32 of the proportional mass loss (since shallow organic soil is less dense), or a correction factor of 0.80. For non-spruce-dominated fuels, this correction is much smaller but still meaningful:

$$\left(\frac{\text{FFFC}}{\text{FFFL}} \right) = 0.13 \left(\frac{\text{depthofburn}}{\text{pre - fireorganicdepth}} \right) + 0.87 \quad (13)$$

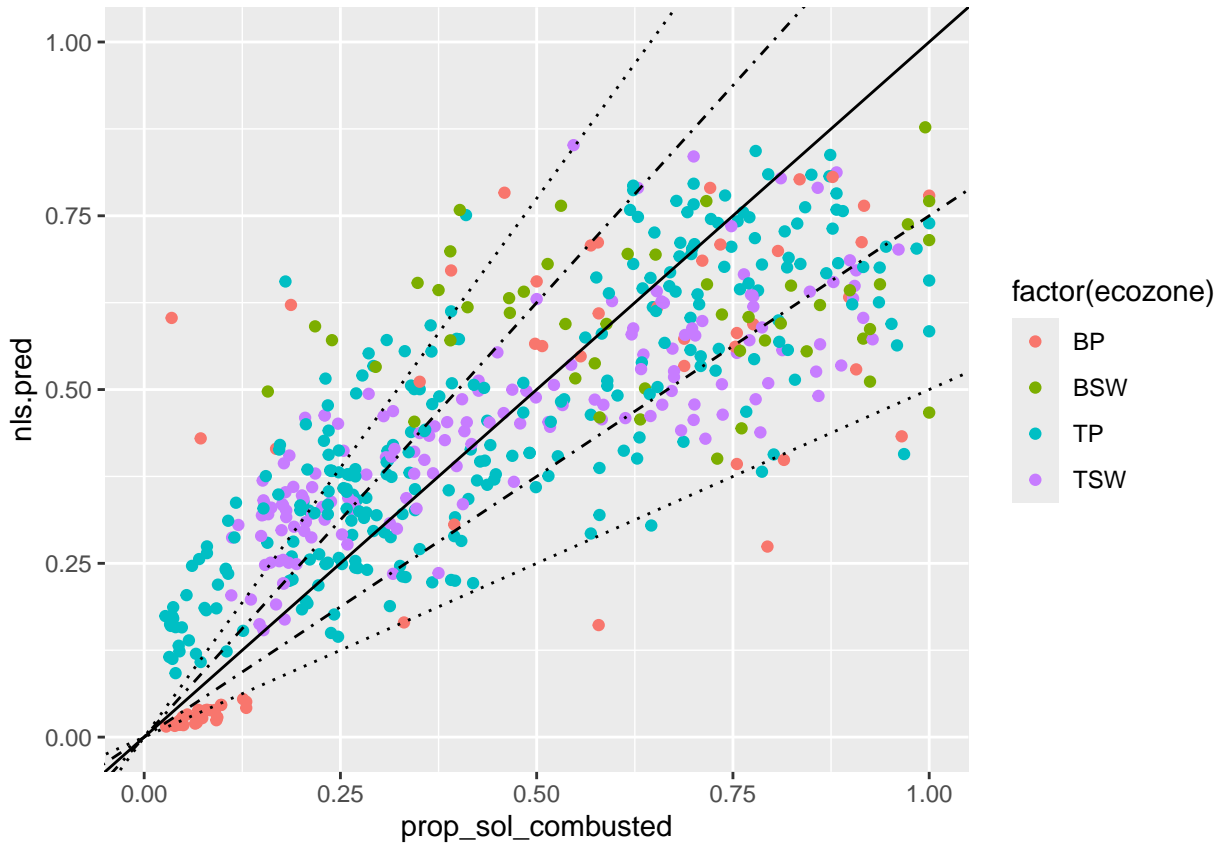
(show perhaps what a few different a values look like?) (also compute the DC value of about half the maximum FBP SFC values too, just for kicks)

For example, using a moderately thick ~12 cm thick organic soil layer, the proportion of consumption as a function of
335 Drought Code using the model above



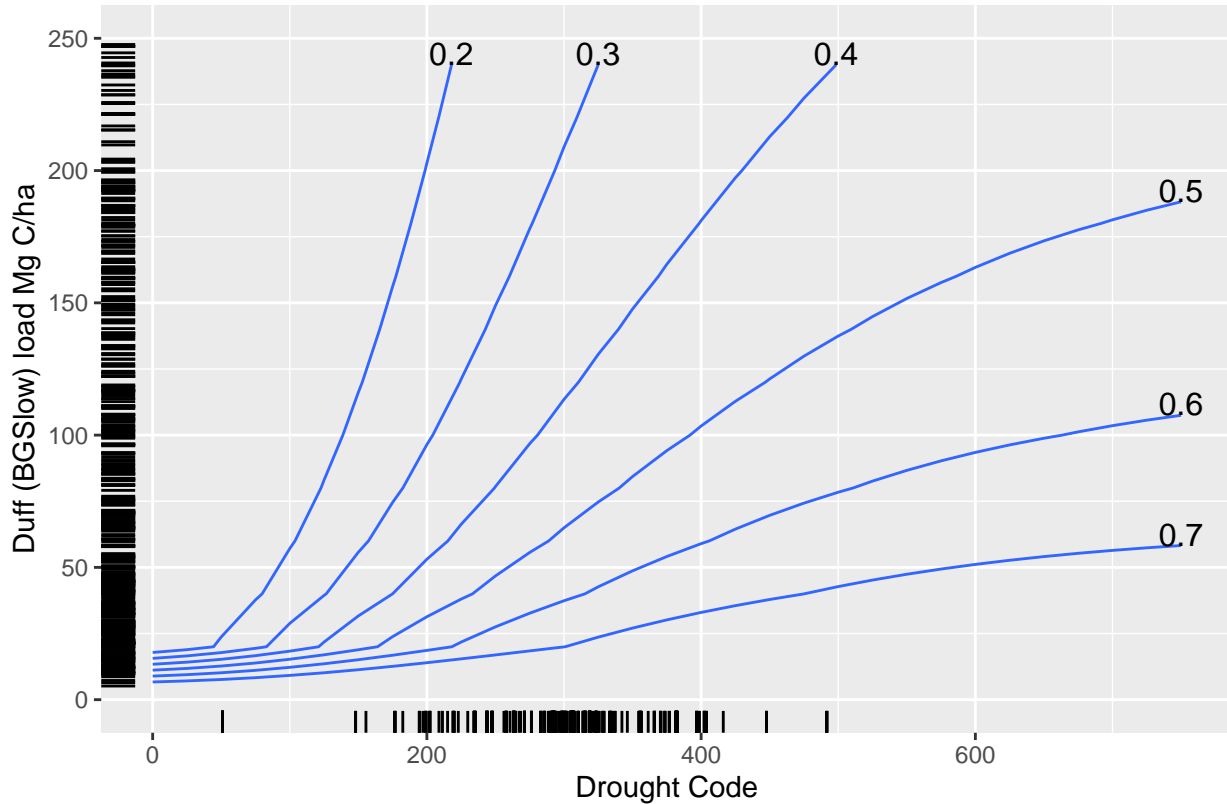
With the parameter constrained NLS fitting, the proportional consumption model for the forest floor has a leave-one-out (conducted at the fire-level, not plot) cross validated r² of ###, and a Mean Percent Error of ###%

```
## Scale for y is already present.  
340 ## Adding another scale for y, which will replace the existing scale.  
## Scale for y is already present.  
## Adding another scale for y, which will replace the existing scale.  
## Scale for x is already present.  
## Adding another scale for x, which will replace the existing scale.
```

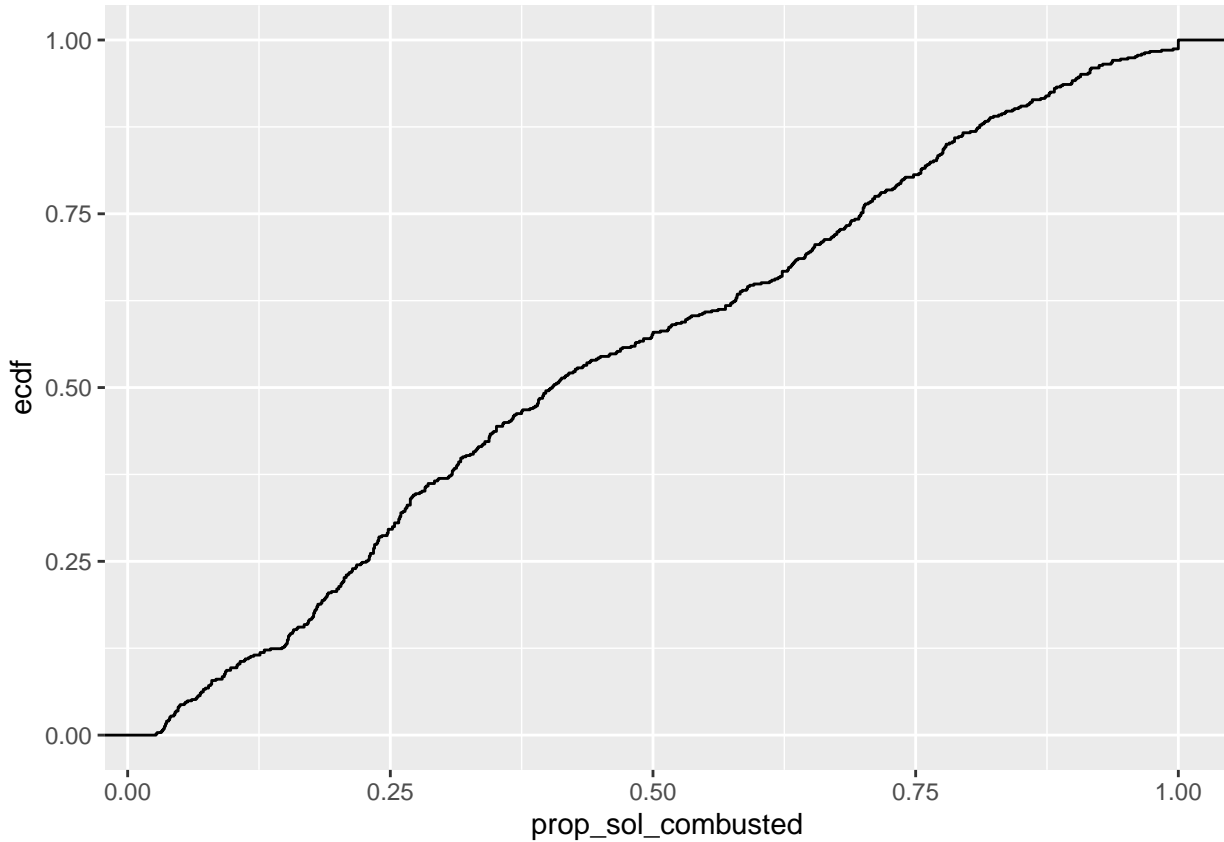


345

Across the entire parameter space of Drought Code and BGSlow pool size, the following isolines of proportional consumption in the model can be plotted:



Isoline contours of equal organic soil layer consumption fraction as a function of Drought Code and the organ



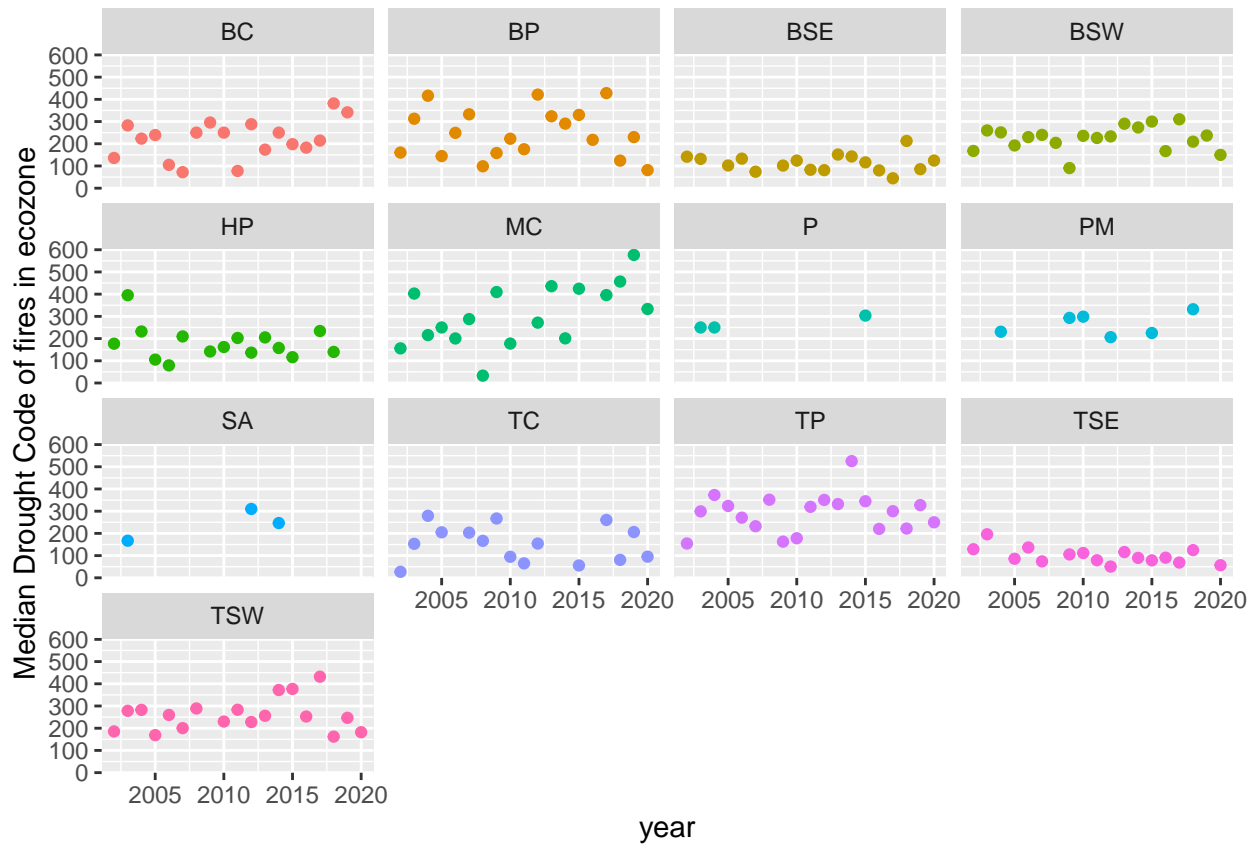
350 5.0.1 Boreal Cordillera modelling

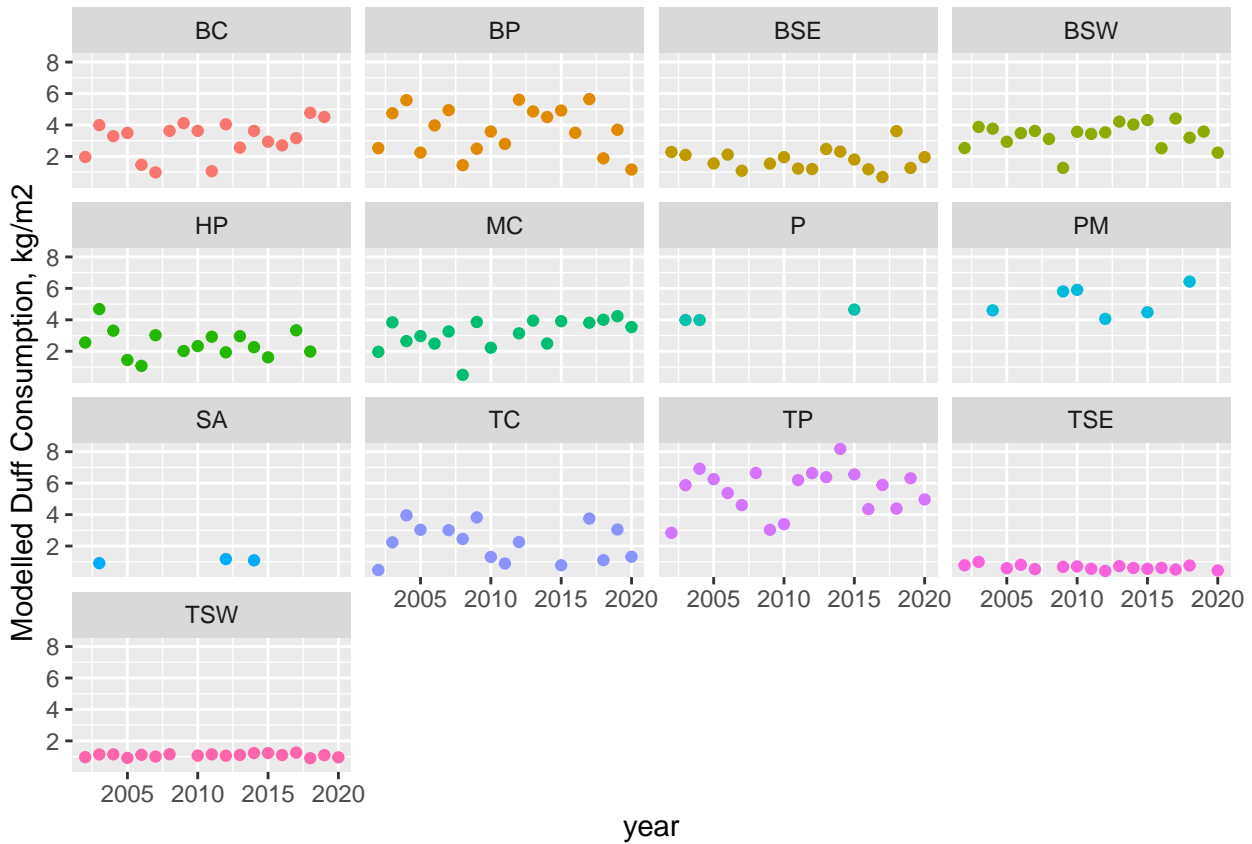
For the Boreal Cordillera, a simple linear model on the logit-transformed data was found to be the best performing model for estimating soil organic consumption proportion:

$$\text{logit} \left(\frac{FFFC}{FFFL} \right) = (0.00257 * DC) + (-0.54 * \log_e(BGSlow)) + 2.17 \quad (14)$$

Despite the presence of a fixed intercept term, the strong inverse dependence on the natural logarithm of the BGSlow pool size (FFFL) results in zero proportional consumption when Drought Code is equal to zero.
355

6 Appendix C: annual variability in observed Drought Code during wildfire spread, and impact on ecozone-level average forest floor emissions





360 7 Appendix D: Representative photos

Photos of: (1) partial litter consumption; (2) partial vs full duff consumption; (3) mortality but not consumption of understory trees with live overstory; (4) mortality but not consumption of overstory trees; (5) mixedwood severity example showing consumption of broadleaf foliage; (6) woody debris consumption; (7) snag preferential consumption relative to little to no bole consumption in live trees

365 Give lat/long, year, ecozone, severity class, and leading spp for each photo, maybe other relevant metrics? From some of the experimental fires mostly??

8 Appendix E: List of Resprouting Hardwoods of Canada

Alnus spp. Arbutus men. Betula all. Betula pap. Betula pop. Fraxinus ame. Fraxinus nig. Fraxinus pen. Populus bal. Populus gra. Populus tre. Populus tri. Quercus spp. Salix spp.

370 #Parking Lot

```

#### table with rows are CBM pools, columns (paird) are obs
#### and modelled exp fires

#### fires that would work:

375 #### ICFME (SW TP High); Sharpsands 2007 (SW BSE High),
#### Lafoe (HW BSE Low), CWS C-7 burns (SW MC Mod), Carrot
#### lake (SW MC High)

380 #### variables specifically measured during an experimental
#### fire, in the verbiage of the fire DMs:
exp.fire.table.defs <- c("SW.CFB", "HW.CFB", "SW.Mort", "HW.Mort",
                         "SW.SubMerch.Mort", "HW.SubMerch.Mort", "SmTree.Mort", "SW.Snag.Comb.Frac",
                         "HW.Snag.Comb.Frac", "MedDOM.Comb.Frac", "Duff.consump.frac")

385 ## then, take the list above, and look up the same row but
## the column 'Plain.Language.Name' in FireDMTableDefs.csv:
## exp.fire.table.labels <-

390 ## note that Duff.consump.frac is an ecozone variable, not
## in FireDMTableDefs.csv

## list of all possible CBM pools measured during an
## experimental fire:
395 exp.fire.pools <- c("Softwood Foliage", "Softwood Other", "Aboveground Very Fast DOM",
                      "Aboveground Fast DOM", "Medium DOM", "Aboveground Slow DOM",
                      "Softwood Stem Snag", "Hardwood Other", "Hardwood Stem Snag")

## fun idea: ternary plots of live vs combusted vs dead
400 #### for each of these fires, modelled vs observed?
#### https://cran.r-project.org/web/packages/Ternary/vignettes/Ternary.html
#### with the colour being the fuel type/leading spp and
#### size being total emissions? can we draw lines in
#### between pairs of mod vs obs in that package? TernaryApp
405 #### function in the package should apparently let you draw

```

```
### connected points?
```

. This article was produced from an RMarkdown document with underlying data, available at <https://github.com/nrcan-cfs-fire/FireDMs>

Appendix A: List of fluxes and corresponding fire-related plain-language summary

A1 Option 1

- 410 If you sorted all figures and tables into the sections of the text, please also sort the appendix figures and appendix tables into the respective appendix sections. They will be correctly named automatically.

A2 Option 2

If you put all figures after the reference list, please insert appendix tables and figures after the normal tables and figures.

- \appendixfigures needs to be added in front of appendix figures \appendixtables needs to be added in front of
415 appendix tables

Please add \clearpage between each table and/or figure. Further guidelines on figures and tables can be found below. Regarding figures and tables in appendices, the following two options are possible depending on your general handling of figures and tables in the manuscript environment: To rename them correctly to A1, A2, etc., please add the following commands in front of them:

- 420 . Thompson and Whitman contributed to the concept and code design with the assistance of Hanes, Hudson

. The authors declare no competing interests.

. The algorithm and results presented only apply to boreal and temperate forest ecosystems where sufficient ground plots of fire severity are available. As a data-driven model, this framework is not suitable for other ecosystems nor agricultural or forestry biomass burning practices.

. Thanks to (insert names here)

- Angers, V. A., Gauthier, S., Drapeau, P., Jayen, K., Bergeron, Y., Angers, V. A., Gauthier, S., Drapeau, P., Jayen, K., and Bergeron, Y.: Tree mortality and snag dynamics in North American boreal tree species after a wildfire: a long-term study, *International Journal of Wildland Fire*, 20, 751–763, <https://doi.org/10.1071/WF10010>, publisher: CSIRO PUBLISHING, 2011.
- Barber, Q. E., Jain, P., Whitman, E., Thompson, D., Guindon, L., Parks, S. A., Wang, X., Hethcoat, M., and Parisien, M.: The Canadian Fire Spread Dataset, <https://doi.org/10.17605/OSF.IO/F48RY>.
- Benscoter, B. W., Thompson, D. K., Waddington, J. M., Flannigan, M. D., Wotton, B. M., Groot, W. J. d., and Turetsky, M. R.: Interactive effects of vegetation, soil moisture and bulk density on depth of burning of thick organic soils, *International Journal of Wildland Fire*, 20, 418–429, <https://doi.org/10.1071/WF08183>, 2011.
- Bernier, P. Y., Gauthier, S., Jean, P.-O., Manka, F., Boulanger, Y., Beaudoin, A., and Guindon, L.: Mapping Local Effects of Forest Properties on Fire Risk across Canada, *Forests*, 7, 157, <https://doi.org/10.3390/f7080157>, 2016.
- Bona, K. A., Shaw, C., Thompson, D. K., Hararuk, O., Webster, K., Zhang, G., Voicu, M., and Kurz, W. A.: The Canadian model for peatlands (CaMP): A peatland carbon model for national greenhouse gas reporting, *Ecological Modelling*, 431, 109 164, <https://doi.org/10.1016/j.ecolmodel.2020.109164>, 2020.
- Brown, J. K. and DeByle, N. V.: Fire damage, mortality, and suckering in aspen, *Canadian Journal of Forest Research*, 17, 1100–1109, <https://doi.org/10.1139/x87-168>, publisher: NRC Research Press, 1987.
- Chen, J., Anderson, K., Pavlovic, R., Moran, M. D., Englefield, P., Thompson, D. K., Munoz-Alpizar, R., and Landry, H.: The FireWork v2.0 air quality forecast system with biomass burning emissions from the Canadian Forest Fire Emissions Prediction System v2.03, *Geoscientific Model Development*, 12, 3283–3310, <https://doi.org/10.5194/gmd-12-3283-2019>, 2019.
- de Groot, W., Pritchard, J., and Lynham, T.: Forest floor fuel consumption and carbon emissions in Canadian boreal forest fires, *Canadian Journal of Forest Research*, 39, 367–382, <https://doi.org/10.1139/X08-192>, 2009.
- Group, F. C. F. D. R.: Development and structure of the Canadian Forest Fire Behavior Prediction System, vol. ST-X-3, Forestry Canada, <https://cfs.nrcan.gc.ca/publications?id=10068>, 1992.
- Hall, R. J., Freeburn, J. T., Groot, W. J. d., Pritchard, J. M., Lynham, T. J., Landry, R., Hall, R. J., Freeburn, J. T., Groot, W. J. d., Pritchard, J. M., and et al.: Remote sensing of burn severity: experience from western Canada boreal fires, *International Journal of Wildland Fire*, 17, 476–489, <https://doi.org/10.1071/WF08013>, 2008.
- Hall, R. J., Skakun, R. S., Metsaranta, J. M., Landry, R., Fraser, R. H., Raymond, D., Gartrell, M., Decker, V., and Little, J.: Generating annual estimates of forest fire disturbance in Canada: the National Burned Area Composite, *International Journal of Wildland Fire*, <https://doi.org/10.1071/WF19201>, 2020.
- Hanes, C. C., Wang, X., Jain, P., Parisien, M.-A., Little, J. M., and Flannigan, M. D.: Fire-regime changes in Canada over the last half century, *Canadian Journal of Forest Research*, 49, 256–269, <https://doi.org/10.1139/cjfr-2018-0293>, 2019.
- Hanes, C. C., Wang, X., Groot, W. J. d., Hanes, C. C., Wang, X., and Groot, W. J. d.: Dead and down woody debris fuel loads in Canadian forests, *International Journal of Wildland Fire*, 30, 871–885, <https://doi.org/10.1071/WF21023>, publisher: CSIRO PUBLISHING, 2021.
- Hayden, K., Li, S.-M., Liggio, J., Wheeler, M., Wentzell, J., Leithead, A., Brickell, P., Mittermeier, R., Oldham, Z., Mihele, C., Staebler, R., Moussa, S., Darlington, A., Steffen, A., Wolde, M., Thompson, D., Chen, J., Griffin, D., Eckert, E., Ditto, J., He, M., and Gentner, D.: Reconciling the total carbon budget for boreal forest wildfire emissions using airborne observations, *Atmospheric Chemistry and Physics Discussions*, pp. 1–62, <https://doi.org/10.5194/acp-2022-245>, publisher: Copernicus GmbH, 2022.

- Hessburg, P. F., Miller, C. L., Parks, S. A., Povak, N. A., Taylor, A. H., Higuera, P. E., Prichard, S. J., North, M. P., Collins, B. M., Hurteau, M. D., Larson, A. J., Allen, C. D., Stephens, S. L., Rivera-Huerta, H., Stevens-Rumann, C. S., Daniels, L. D., Gedalof, Z., Gray, R. W., Kane, V. R., Churchill, D. J., Hagmann, R. K., Spies, T. A., Cansler, C. A., Belote, R. T., Veblen, T. T., Battaglia, M. A., Hoffman, C., Skinner, C. N., Safford, H. D., and Salter, R. B.: Climate, Environment, and Disturbance History Govern Resilience of Western North American Forests, *Frontiers in Ecology and Evolution*, 7, <https://doi.org/10.3389/fevo.2019.00239>, 2019.
- Hood, S. and Lutes, D.: Predicting Post-Fire Tree Mortality for 12 Western US Conifers Using the First Order Fire Effects Model (FOFEM), *Fire Ecology*, 13, 66–84, <https://doi.org/10.4996/fireecology.130290243>, 2017.
- Jain, P., Barber, Q. E., Taylor, S. W., Whitman, E., Castellanos Acuna, D., Boulanger, Y., Chavardès, R. D., Chen, J., Englefield, P., Flannigan, M., and et al.: Drivers and Impacts of the Record-Breaking 2023 Wildfire Season in Canada, *Nature Communications*, 15, 6764, <https://doi.org/10.1038/s41467-024-51154-7>, 2024.
- Kurz, W. A., Apps, M., Banfield, E., and Stinson, G.: Forest carbon accounting at the operational scale, *The Forestry Chronicle*, 78, 672–679, <https://doi.org/10.5558/tfc78672-5>, 2002.
- Letang, D. and de Groot, W.: Forest floor depths and fuel loads in upland Canadian forests, *Canadian Journal of Forest Research*, 42, 1551–1565, <https://doi.org/10.1139/x2012-093>, 2012.
- 475 McAlpine, R. S.: Testing the Effect of Fuel Consumption on Fire Spread Rate, *International Journal of Wildland Fire*, 5, 143–152, <https://doi.org/10.1071/wf9950143>, 1995.
- Michaletz, S. T. and Johnson, E. A.: A heat transfer model of crown scorch in forest fires, *Canadian Journal of Forest Research*, 36, 2839–2851, <https://doi.org/10.1139/x06-158>, publisher: NRC Research Press, 2006.
- 480 Parisien, M.-A., Barber, Q. E., Hirsch, K. G., Stockdale, C. A., Erni, S., Wang, X., Arseneault, D., and Parks, S. A.: Fire deficit increases wildfire risk for many communities in the Canadian boreal forest, *Nature Communications*, 11, 1–9, <https://doi.org/10.1038/s41467-020-15961-y>, 2020.
- Pérez-Izquierdo, L., Clemmensen, K. E., Strengbom, J., Nilsson, M.-C., and Lindahl, B.: Quantification of tree fine roots by real-time PCR, *Plant and Soil*, 440, 593–600, <https://doi.org/10.1007/s11104-019-04096-9>, 2019.
- 485 Simon, H., Beck, L., Bhave, P. V., Divita, F., Hsu, Y., Luecken, D., Mobley, J. D., Pouliot, G. A., Reff, A., Sarwar, G., and Strum, M.: The development and uses of EPA's SPECIATE database, *Atmospheric Pollution Research*, 1, 196–206, <https://doi.org/10.5094/APR.2010.026>, 2010.
- Simpson, I. J., Akagi, S. K., Barletta, B., Blake, N. J., Choi, Y., Diskin, G. S., Fried, A., Fuelberg, H. E., Meinardi, S., Rowland, F. S., Vay, S. A., Weinheimer, A. J., Wennberg, P. O., Wiebring, P., Wisthaler, A., Yang, M., Yokelson, R. J., and Blake, D. R.: Boreal forest fire emissions in fresh Canadian smoke plumes: C₁-C₁₀ volatile organic compounds (VOCs), CO₂, CO, NO₂, NO, HCN and CH₃CN, *Atmospheric Chemistry and Physics*, 11, 6445–6463, <https://doi.org/10.5194/acp-11-6445-2011>, publisher: Copernicus GmbH, 2011.
- 490 Skakun, R., Castilla, G., Metsaranta, J., Whitman, E., Rodrigue, S., Little, J., Groenewegen, K., and Coyle, M.: Extending the National Burned Area Composite Time Series of Wildfires in Canada, *Remote Sensing*, 14, 3050, <https://doi.org/10.3390/rs14133050>, 2022.
- Stinson, G., Thandi, G., Aitkin, D., Bailey, C., Boyd, J., Colley, M., Fraser, C., Gelhorn, L., Groenewegen, K., Hogg, A., and et al.: A new approach for mapping forest management areas in Canada, *The Forestry Chronicle*, 95, 101–112, <https://doi.org/10.5558/tfc2019-017>, 2019.
- Stocks, B. J., Mason, J. A., Todd, J. B., Bosch, E. M., Wotton, B. M., Amiro, B. D., Flannigan, M. D., Hirsch, K. G., Logan, K. A., Martell, D. L., and et al.: Large forest fires in Canada, 1959–1997, *Journal of Geophysical Research: Atmospheres*, p. FFR 5–12, <https://doi.org/10.1029/2001JD000484>, 2002.

- 500 Strong, W. L. and La Roi, G. H.: Root density-soil relationships in selected boreal forests of central Alberta, Canada, *Forest Ecology and Management*, 12, 233–251, [https://doi.org/10.1016/0378-1127\(85\)90093-3](https://doi.org/10.1016/0378-1127(85)90093-3), 1985.
- White, J. C., Wulder, M. A., Hermosilla, T., Coops, N. C., and Hobart, G. W.: A nationwide annual characterization of 25 years of forest disturbance and recovery for Canada using Landsat time series, *Remote Sensing of Environment*, 194, 303–321, <https://doi.org/10.1016/j.rse.2017.03.035>, 2017.
- 505 Whitman, E., Parisien, M.-A., Thompson, D. K., Hall, R. J., Skakun, R. S., and Flannigan, M. D.: Variability and drivers of burn severity in the northwestern Canadian boreal forest, *Ecosphere*, 9, e02128, <https://doi.org/10.1002/ecs2.2128>, 2018.
- Whitman, E., Parisien, M.-A., Holsinger, L. M., Park, J., and Parks, S. A.: A method for creating a burn severity atlas: an example from Alberta, Canada, *International Journal of Wildland Fire*, <https://doi.org/10.1071/WF19177>, 2020.